


SEISMIC VELOCITIES IN CARBONATE ROCKS

Z. WANG W.K. HIRSCH G. SEDGWICK

this article begins on the next page 



JCPT91-02-09

RESERVOIR ENGINEERING

Seismic velocities in carbonate rocks

ZHIJING WANG

Core Laboratories

W. KEITH HIRSCH

Western Geophysical

and

GEORGE SEDGWICK

Alberta Research Council

ABSTRACT

Seismic velocities were measured in the laboratory vs pressure, temperature, and saturation on over 80 cores from various carbonate reservoirs in Alberta, using an ultrasonic pulse transmission method. Porosity, permeability, electrical properties, and capillary pressure were also measured in order to characterize the pore systems. All the measured data and other information are compiled into a database.

The results show that both permeabilities and seismic velocities are related to the porosities of the cores, although the data are scattered. Liquid saturation (e.g. oil and water) increases the compressional velocity but has only nominal effect on the shear velocity. The magnitude of the increase in compressional velocities with liquid saturation is dependent upon the pore geometry of the rocks, reservoir pressure, as well as the distribution and properties of the saturating fluids.

The velocity data are also fit to the time-average equation and the Gassmann equation. The results are usually unsatisfactory, which means that the time-average equation used in sonic log interpretation is inadequate. For log interpretation, it might be desirable to establish a porosity-velocity relationship specific to carbonate reservoirs, instead of using the time-average equation. Furthermore, the Gassmann equation does not adequately explain the laboratory results.

In most of the cores measured, the compressional velocities increase by more than 5% with oil saturation, with a subsequent decrease by over 5% when flooded with a hydrocarbon solvent. This suggests that seismic monitoring of injected gases and hydrocarbon solvent in carbonate reservoirs should be possible.

Introduction

Seismic properties of rocks are very important to petroleum exploration and production. In seismic exploration, velocity and density contrast between two rock layers causes reflection of seismic waves at the interface. The reflected seismic waves bring out information on the structure of the earth's crust, so that the seismic interpreter can look for potential hydrocarbon traps from the

seismic profile. In the process of seismic exploration, a thorough understanding of seismic velocities in rocks plays a vital role in the success of seismic methods.

In recent years, seismic methods have found other applications with success in petroleum production assessment, reservoir characterization, and enhanced oil recovery (EOR) and production monitoring. In seismic monitoring applications, the velocity contrast caused by various EOR and production processes is the physical basis of the method. Laboratory results have shown that large velocity decreases are found in heavy oil sands as temperature increases⁽¹⁻³⁾, in oil-saturated rocks when flooded with carbon dioxide (CO₂)^(6,7) and in oil-saturated rocks when flooded with gas and hydrocarbon solvent^(8,9). Furthermore, laboratory results also show large differences between the compressional velocities in gas- and liquid- (e.g. water or oil) saturated rocks⁽¹⁰⁾. These results open the door for using seismic methods to monitor EOR and production processes.

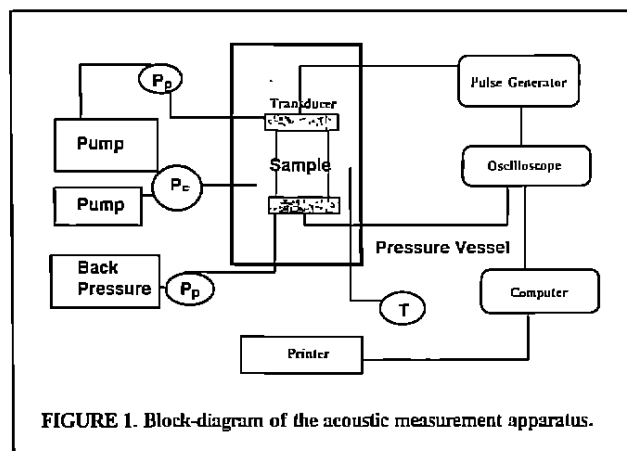
In the literature, most of the seismic velocity data were measured in sandstones and sand. Little has been published on seismic properties of carbonate rocks. Rafavich *et al.*⁽¹¹⁾ measured 93 Mission Canyon formation carbonate cores from four wells in the Williston basin field, North Dakota, which appears to be the only systematic study of seismic velocities in carbonates. In this study, more than 80 cores were selected from over ten carbonate reservoirs in Alberta and systematic studies were performed on seismic velocities of these carbonate rocks, as well as other properties such as petrographic image analysis, porosity and permeability, electrical properties, and capillary pressure.

The primary objective of this study is to determine if there is enough velocity contrast between the oil-saturated and solvent-flooded rocks to apply seismic methods to monitoring of the hydrocarbon solvent flooding processes. This monitoring would enable the engineer to track the solvent bank and to map the solvent-flooded zones in reservoirs.

The secondary objective of this study is to characterize properties of carbonate rocks of Alberta reservoirs. Cores were selected to cover a wide range of porosities and permeabilities so that the effect of porosity on seismic velocities and other properties could be studied.

In this paper, acoustic velocities in the measured cores vs porosity, pressure, and oil-saturation at reservoir temperature are presented. The effect of hydrocarbon solvent flooding, along with that of the pentane and waterflooding, on the seismic velocities

Keywords: Seismic velocities, carbonates, EOR monitoring, Miscible displacement, Immiscible displacement.



is analyzed and discussed. In order to verify measured data, theoretical analysis is performed on the velocities using the time-average equation, Gassmann equation, and Toksoz *et al.* model. Finally, some applications of the results are discussed.

Experiments

Apparatus

The apparatus employed for measuring acoustic velocities in rocks consists of an electronics system and a mechanical package. The electronics system includes a high-voltage pulse generator, a digital oscilloscope, a computer, and a graphics printer. The mechanical package is composed of a hydrostatic pressure vessel, a confining-pressure pump, a pore-pressure pump, a back pressure regulator, a pair of 500 kHz piezoelectric transducers, a temperature controller, and pressure and temperature gauges (Fig. 1).

Ultrasonic pulses generated by the pulse generator are converted to mechanical vibration by the transmitting piezoelectric transducer. After travelling through the rock sample, the mechanical (elastic) waves are converted back to an electrical signal by the receiving transducer. The travel-time of the acoustic waves can be measured on the digital oscilloscope so that the velocities are calculated by

$$V_{p,s} = \frac{L}{\Delta t} \quad (1)$$

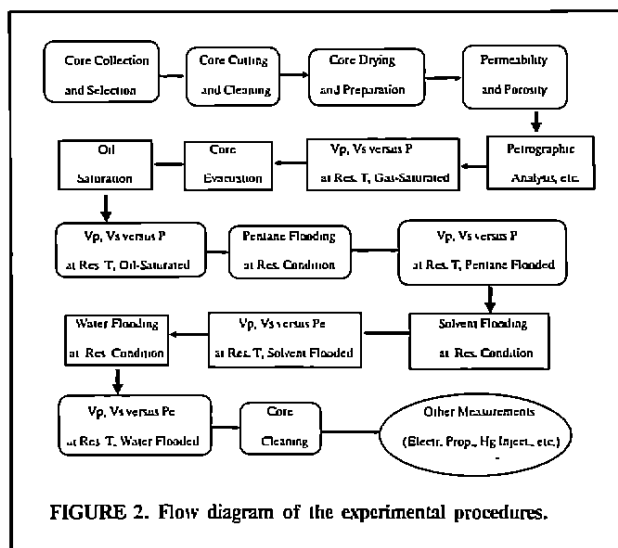
where p,s represent compressional and shear waves, L and Δt are the sample length and travel-time, respectively. The acoustic waveforms are recorded on the computer's hard-disk for later analyses.

Experimental Procedure

Cores, collected from various carbonate reservoirs in Alberta, Canada were cleaned in toluene/methanol extractors for about one week and cut to appropriate length for measurements. Surface vugs were filled with high-strength epoxy or a special cement. For very vuggy samples, full-diameter cores (8.9 cm or 3.5 in.) were used for the measurements. For homogeneous cores, plugs of 3.8 cm (1.5 in.) in diameter were prepared and measured. The sample lengths ranged from 10 cm to 18 cm (4 in. to 7 in.) for full-diameter cores and from 5 cm to 10 cm (2 in. to 4 in.) for core plugs.

After cleaning, the samples were analyzed for mineral composition and pore structure and measured for porosity and permeability. The two end-surfaces of all the samples were finely machined to parallel and then the samples were dried in an oven for five days at about 70°C.

Prior to measuring acoustic velocities, the sample was jacketed in a high-temperature rubber sleeve to separate pore pressure from overburden (hydrostatic) pressure and then loaded into the pressure vessel. Overburden pressure was increased to 48.3 MPa (7000 psi) and then lowered to 6.9 MPa (1000 psi) with zero pore (fluid) pressure to eliminate any possible velocity hysteresis. Temperature was raised to reservoir temperature through a built-in heater.



When the rock sample was heated up and temperature had reached equilibrium (it usually took 2 to 3 hours), velocities in the dry (with air in the pores) rock were measured vs overburden pressure. Afterwards, the rock sample was evacuated and saturated with oil. The sample was left overnight for saturation at overburden pressure 20.7 MPa (3000 psi) and pore pressure 13.8 MPa (2000 psi).

After the velocities were measured in the oil-saturated sample, 5 to 15 pore volumes of normal pentane (C_5H_{12}) were flooded through the sample at 0.5 cc/minute. Pore pressure was controlled at 13.8 MPa (2000 psi) by the back-pressure regulator. The pentane-flooded sample was left for about 16 hours before the velocities were measured.

The pentane-flooded core sample was next flooded with the hydrocarbon solvent at a constant overburden pressure of 20.7 MPa and pore pressure of 13.8 MPa. Sixteen hours later, the velocities were measured again in the core sample.

The sample was finally flooded with fresh water at the same conditions as in the pentane and solvent displacements. The water-flooded sample was left in the pressure vessel for about 16 hours before the velocities were measured. A block diagram of the experimental procedures is shown in Figure 2.

Properties of the Rocks and Fluids

Rocks

Over 80 rock samples were collected from over 10 oil-producing carbonate reservoirs in Alberta. These rock samples consist of 41 limestones and 34 dolomites, with the rest being of mixed lithology. The porosity ranges from 0.03 to 0.21, permeability from 0.2 mD to 3800 mD, and grain density from 2700 kg/m³ to 2850 kg/m³. The reservoir temperature and depth for these rock samples range from 21°C to 105°C and from 500 m to 3100 m, respectively.

Figure 3 shows the porosity-permeability relationship for the measured rock samples at ambient condition. The solid line in the figure

$$\text{Log } K = -0.950 + 15.213\phi \quad (2)$$

represents the least-square best-fit to the data, where K and ϕ are permeability and porosity, respectively. The measured permeability data vs porosity deviate substantially from the best-fit line, with the correlation factor being about 0.4. However, the trend indicates that permeability increases exponentially with increasing porosity.

Pore Fluids

The pore fluids used in the experiments are air, Carnation oil, normal pentane, a hydrocarbon solvent, and fresh water. Air was

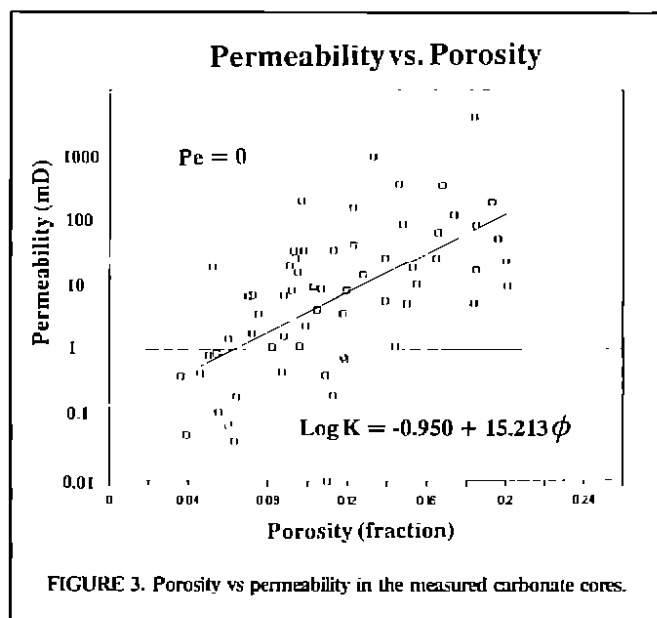


TABLE 1. Physical properties of the pore fluids at 20°C and 1 atmosphere

Fluid	Density (g/cc)	Velocity (m/s)	Viscosity (mPa.s)
Carnation	0.835	1410	17.0
Pentane	0.626	1030	0.24
Solvent	0.42*	—	—
Water	0.997	1492	1.0

*at 20°C and 17.3 MPa.

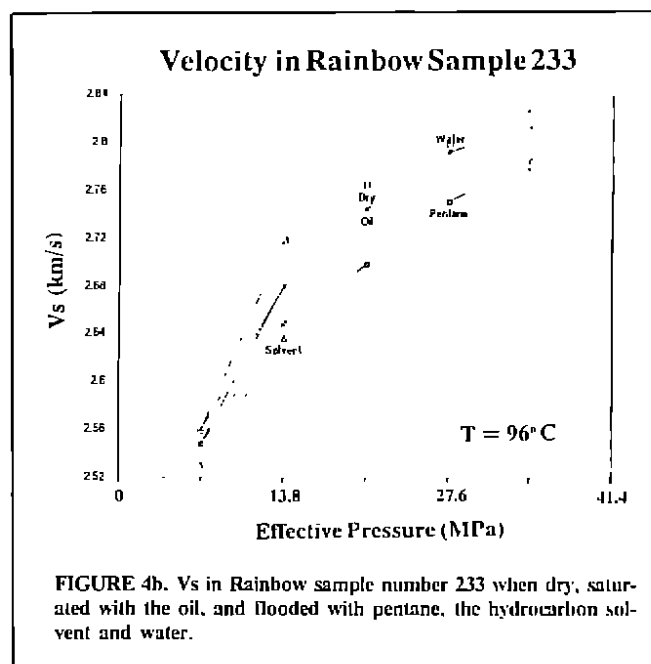
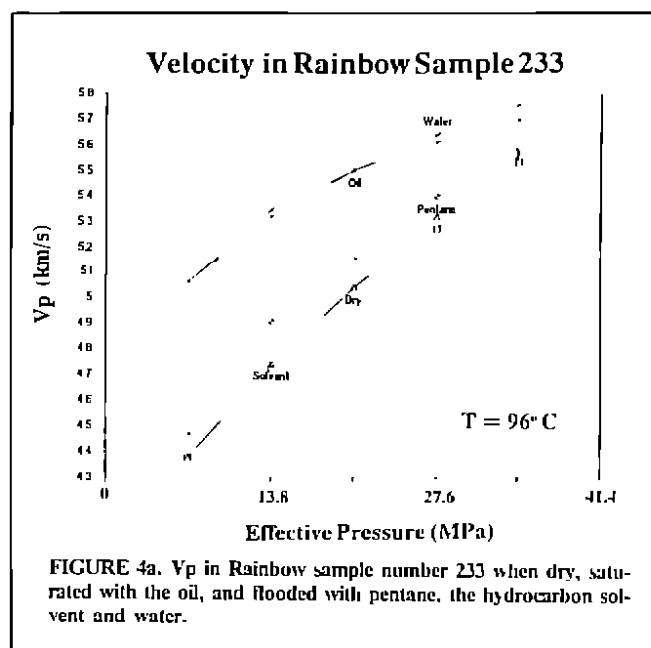
used to simulate natural gas. Carnation oil is a nonpolar white mineral oil with equivalent API gravity of approximately 35 degrees. Normal pentane is a pure hydrocarbon with chemical formula of C_5H_{12} . It was used to simulate extremely light oil (condensate) or heavy hydrocarbon solvent. The hydrocarbon solvent is composed mainly of methane (about 45 vol. %), ethane (about 20 vol. %), propane (20 vol. %), and other hydrocarbons up to heptane (0.74 vol. %). It was collected from an actual hydrocarbon miscible flood pilot. The critical temperature of this hydrocarbon solvent is 56°C at 13.8 MPa (2000 psi). The density and bulk modulus of the solvent at 20°C and 17.3 MPa (2500 psi) are 0.42 g/cc and 19 MPa, respectively. At 89°C and 17.3 MPa, they are 0.30 g/cc and 6.4 MPa, respectively. Physical properties of the pore fluids are listed in Table 1.

Results

V_p and V_s are plotted vs effective pressure (P_e) at reservoir temperature for each core sample when it is dry, saturated with oil, and consecutively flooded with pentane, hydrocarbon solvent, and water. Figures 4 and 5 show, as examples, V_p (Figs. 4a and 5a) and V_s (Figs. 4b and 5b) in sample 233 from the Rainbow reservoir and sample D from the Boundary Lake reservoir. As pressure increases, both V_p and V_s increase, no matter what fluid is in the pores. V_p increases when the air is replaced by oil. The magnitude of this increase depends on pressure and varies among samples. At lower effective pressure, the increase is higher.

When the oil-saturated core sample is flooded with several pore volumes of pentane, V_p decreases (Figs. 4a and 5a). The magnitude of this decrease upon pentane flooding depends on the pressure and temperature of the rock. After the sample is flooded with several pore volumes of hydrocarbon solvent, V_p decreases further, because the hydrocarbon solvent is more compressible than pentane. Finally, the core sample is flooded with fresh water. Most of the gaseous solvent is displaced out of the sample by water so that V_p increases (Figs. 4a and 5a).

Shear velocity (V_s) is not very sensitive to pore fluid changes, because low-viscosity fluids do not support shear stress. When air



in the pores is replaced by oil, V_s can either decrease or increase (Figs. 4b and 5b).

Theoretical Analysis

The experimental results show that oil saturation increases and pentane and solvent floodings decrease the compressional velocities in all the samples. The magnitude of the V_p decreases when the samples are flooded with the hydrocarbon solvent controls whether seismic methods can be used for in-situ monitoring of solvent floods. It is therefore important to analyze our data to see if theory predicts a similar decrease in V_p .

Time-Average Equation

The time-average equations^(1,2) is widely used in sonic log interpretations to derive porosity information from sonic velocities. The equation relates the V_p in a fluid-saturated rock to those in the solid rock matrix and the pore fluid:

$$\frac{1}{V_p} = \frac{1-\phi}{V_m} + \frac{\phi}{V_f} \quad (3)$$

Velocity in Boundary Lake Sample D

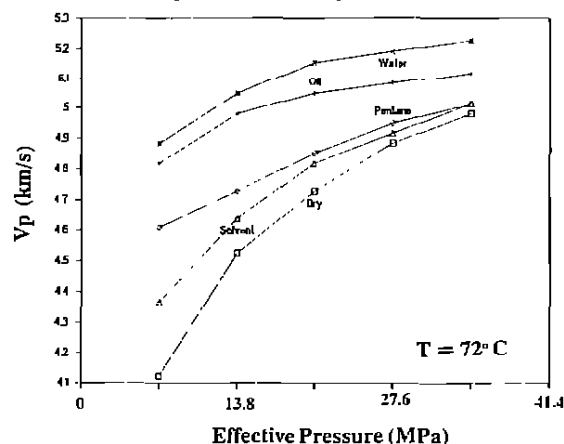


FIGURE 5a. V_p in Boundary Lake sample number D when dry, saturated with the oil, and flooded with pentane, the hydrocarbon solvent and water.

Measured vs Calculated V_p

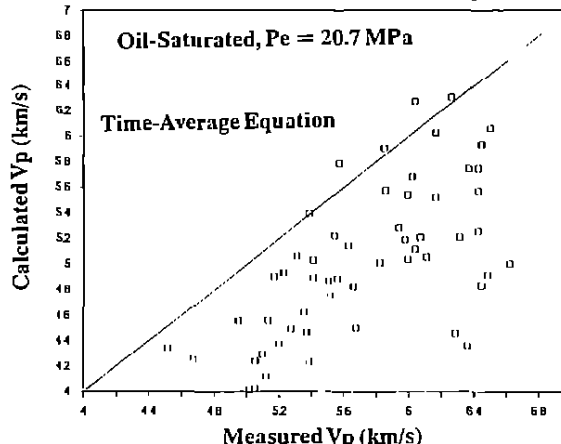


FIGURE 6. Measured vs calculated V_p using the time-average equation in the rocks saturated with oil at 20.7 MPa and reservoir temperature.

Velocity in Boundary Lake Sample D

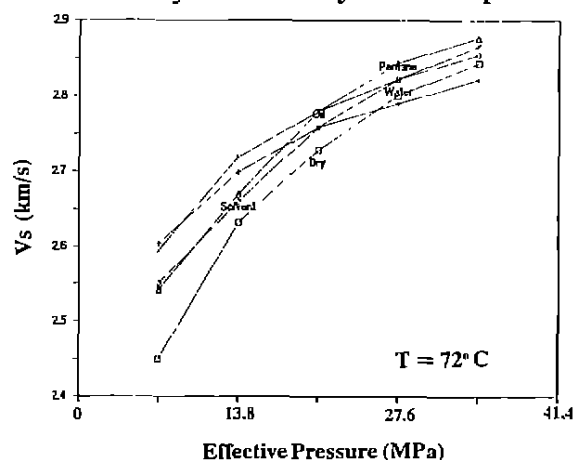


FIGURE 5b. V_s in Boundary Lake sample number D when dry, saturated with the oil, and flooded with pentane, the hydrocarbon solvent and water.

Measured vs Calculated V_p

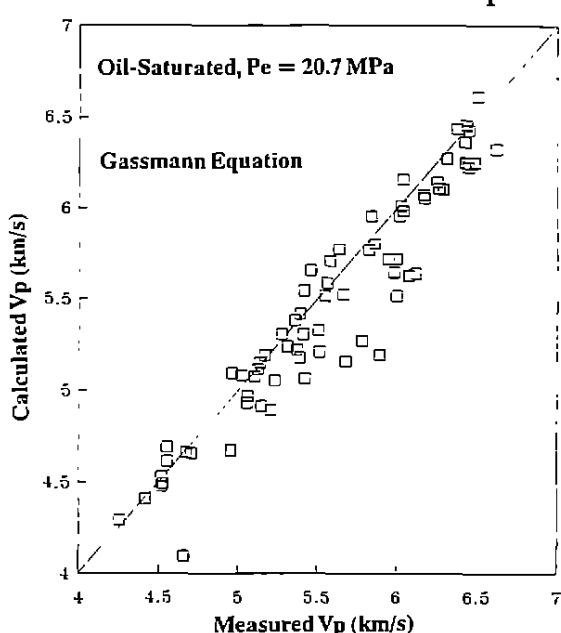


FIGURE 7. Measured vs calculated V_p using the Gassmann equation in rocks saturated with the oil.

where V_m and V_f are the compressional velocities in the solid rock matrix and the pore fluid, respectively, and ϕ is porosity.

Figure 6 shows the measured vs the calculated V_p using the time-average equation in the oil-saturated rocks at 20.7 MPa effective pressure, with an assumed V_m of 7000 m/s. The calculated V_p in most rocks is lower than the measured V_p , typically by 3% to 15% but up to 31%. Only in a few samples is the calculated V_p close to the measured V_p . This difference is also reflected in sonic log interpretation charts. For example, in Schlumberger's log interpretation charts (1986 edition, page 17), the field-observed sonic velocities in limestones and dolomites are higher than the calculated velocities using the time-average equation (by up to 15%) except at very low and high porosities. To minimize the deviation between the calculated and measured V_p in oil-saturated rocks, a combination of either $V_m = 8200$ m/s or 8500 m/s and the measured V_f or $V_m = 7000$ m/s and $V_f = 2050$ m/s is required, both of which are unrealistic.

This simple time-average equation does not work for most rocks (especially carbonate rocks) because it does not realistically model wave propagation in the rock. When the velocity of the pore fluid becomes very low (e.g. velocities in the hydrocarbon solvent or pentane), the equation breaks down and gives very low V_p . This

equation works best in clean (clay-free) sandstones with porosity ranging from 15% to 25%.

Gassmann Equation and Biot Theory

Gassmann developed an equation⁽¹³⁾ which relates the moduli of the fluid-saturated porous medium to those of the frame, grains, and the pore fluid. The Gassmann equation can be used to calculate velocities in fluid-saturated rocks at essentially zero frequency, if the velocities in the dry rock and other parameters are known. The equations are:

$$V_p^2 = \frac{1}{\rho_c} \left[\frac{(K_s - K_d)^2}{K_s \left[1 - \phi - \left(\frac{K_d}{K_i} \right) + \phi \left(\frac{K_s}{K_f} \right) \right]} + K_d + \frac{4}{3} \mu \right] \dots (4)$$

Calculated Vp, Gassmann vs Toksoz

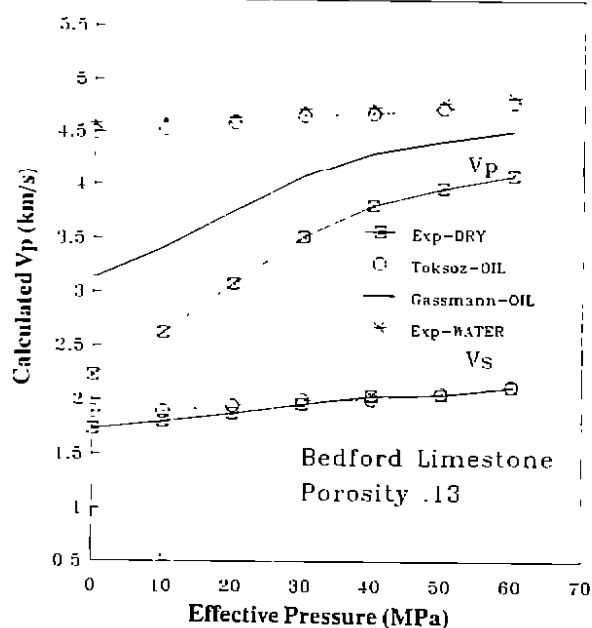


FIGURE 8a. Comparison of the calculated Vp in Bedford limestone using the Gassmann equation and the Toksoz model, using the pore aspect ratios and distributions given by Toksoz *et al.* (1976).

Calculated Vp, Gassmann vs Toksoz

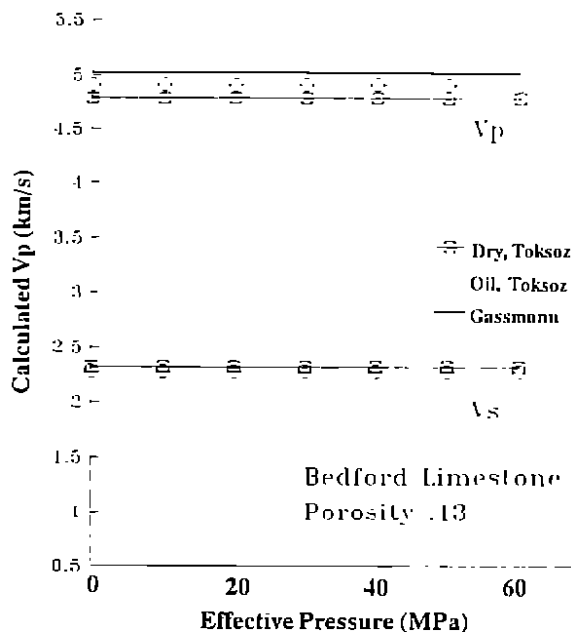


FIGURE 8b. Comparison of the calculated Vp in Bedford limestone using the Gassmann equation and the Toksoz model, using assumed aspect ratios and distributions.

and

$$V_s^2 = \frac{\mu}{\rho_c} \quad (5)$$

where

$$K_d = \rho_d \left(V_{pd}^2 - \frac{4}{3} V_{sd}^2 \right) \quad (6)$$

and

$$\mu = \rho_d V_{sd}^2 \quad (7)$$

are the bulk and shear moduli of, $\rho_d = (1 - \phi) \rho_s$ is the density of, and V_{pd} and V_{sd} are the compressional and shear wave velocities in, the dry rock, respectively. Other notations are: ϕ , porosity; ρ_s , density of the solid matrix; K_f , bulk modulus of the pore fluid; K_s , bulk modulus of the solid matrix; ρ_f , density of the pore fluid; and $\rho_c = (1 - \phi) \rho_s + \phi \rho_f$, density of the saturated rock.

In the velocity calculations using this Gassmann equation, the K_s value is assumed to be 80 GPa for limestones and 96 GPa for dolomites, K_d and μ are derived from the velocities in the dry rock, K_f is derived from the velocity in the pore fluid, and ρ_c and ϕ are measured in the laboratory.

The calculated Vp using the Gassmann equation follows the measured trend that Vp decreases with increasing porosity. Similar predictions are made for the pentane-, solvent-, and water-flooded cores (figures not shown).

In general, the Gassmann-predicted saturated velocities matched the measured data well. The average difference between the calculated and measured velocities is about 2%. Figure 7 shows that the Gassmann predictions were both lower and higher than the measured values with significant scatter being evident. The disagreements between the calculated and measured velocities can be attributed to the imperfections in the Gassmann model.

Besides the Gassmann equation, Biot theory⁽¹⁴⁾ can also be used to calculate velocities in fluid-saturated rocks. At zero wave frequency, Biot theory is exactly the Gassmann equation. At higher wave frequencies, it relates the bulk modulus of a fluid-saturated rock to those of the dry rock and pore fluid and wave frequency.

However, Biot theory does not predict a strong relationship between velocity and wave frequency: as frequency increases from zero to infinity, velocities increase only by 1% to 3% in most rocks⁽¹⁵⁾. For practical purposes, the Gassmann equation is generally used.

The average difference between the Gassmann-predicted and measured velocities is about 2%, within the expected range of velocity dispersions. Careful examination of the data in Figure 7 shows that while the average difference could be dispersion related, several factors cause this assumption to fail. Dispersion can explain the average misfit between Gassmann-predicted and measured velocity data, but can not reduce the scatter in the data. One-third of the samples have measured velocities being lower than those predicted by as much as 2%. If dispersion is truly the mechanism for the misfit, the measured velocities should be always higher than the calculated velocities. Besides, the measured velocities in some samples are as much as 17% higher than the Gassmann-predicted values. This magnitude of difference is too high to be explained by dispersion alone.

The Gassmann equation does not include any pore geometry information (one of Gassmann's assumptions is that all the pores are connected, i.e. the pore fluid phase is continuous). However, cracks or microfractures contribute most to the compressibility of rocks because they are the most compliant parts of the pore space^(16,17).

Toksoz *et al.* Model

Toksoz *et al.*⁽¹⁸⁾ developed a set of equations based on scattering theory and the Kuster-Toksoz model⁽¹⁹⁾ to calculate velocities in porous rocks. Unlike the time-average and the Gassmann equations, the Toksoz model includes information on pore geometry. For an isotropic medium with random distribution of pores of different aspect ratios and saturated with a fluid (zero shear modulus), the Toksoz equations can be written as (for multi-phase fluid-saturated rocks, the equations are slightly different):

$$\frac{K_s - K}{3K + 4\mu_s} = \frac{K_s - K_f}{9K_s + 12\mu_s} \sum_{m=1}^M c(\alpha_m) T_{ijj}(\alpha_m) \quad (8)$$

$$\frac{\mu_s - \mu}{6\mu(K_s + 2\mu_s) + \mu_s(9K_s + 8\mu_s)} = \frac{\mu_s}{25\mu_s(3K_s + 4\mu_s)} \sum_{m=1}^M c(\alpha_m) \left[\Gamma_{ijj}(\alpha_m) \right]$$

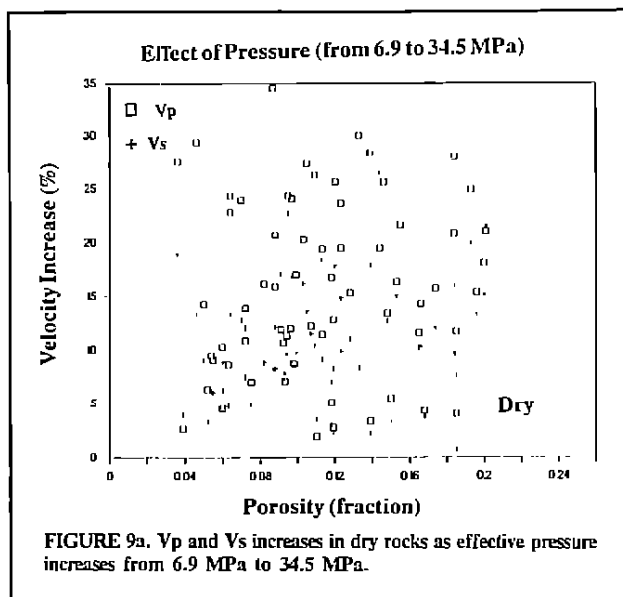


FIGURE 9a. Vp and Vs increases in dry rocks as effective pressure increases from 6.9 MPa to 34.5 MPa.

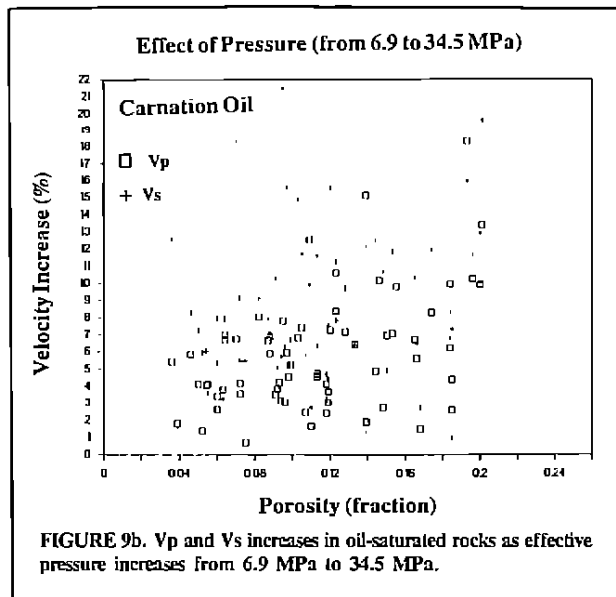


FIGURE 9b. Vp and Vs increases in oil-saturated rocks as effective pressure increases from 6.9 MPa to 34.5 MPa.

$$- \frac{1}{3} T_{ijj}(\alpha_m) \dots \dots \dots (9)$$

$$\varphi = \sum_{m=1}^M c(\alpha_m) \dots \dots \dots (10)$$

and $\rho_c = \rho_s(1 - \varphi) + \varphi\rho_f$, where K and μ denote the bulk and shear moduli of the saturated rock and the subscripts s and f represent the rock matrix and pore fluid, respectively. $c(\alpha_m)$ is the concentration of pores with aspect ratio of α_m . T_{ijj} and T_{ijj} are scalar quantities defined in Toksoz *et al.*⁽¹⁰⁾ as functions of the properties of the rock matrix and pore fluid and aspect ratio α .

In formulating their model, Toksoz *et al.* recognized that standard models could not explain several effects observed in experimental data. These effects included the large velocity increase upon saturation observed in igneous rocks with less than 1% porosity, the occasional shear velocity increase with saturation, and the large velocity changes with pressure in dry rocks, coupled with greatly reduced pressure dependency after saturation. They formulated their model to incorporate pore aspect ratio data into the velocity computation to explain these observations. The model includes pore closure as a function of pressure, which enables the model to compute realistic pressure dependencies in dry rocks.

Toksoz *et al.* tested their model using several examples of published laboratory data. One of these examples was the Bedford limestone velocities measured vs saturation and pressure by Nur and Simmons⁽¹⁰⁾. The computed velocities matched measured velocities almost perfectly for dry and water-saturated Vp and Vs, using assumed aspect ratios (Fig. 8a).

Additionally, the authors computed oil-saturated velocities using the Toksoz model and their published aspect ratios. The oil-saturated velocities are slightly lower than but parallel to the measured water-saturated velocities vs pressure. The dry velocities are strongly dependent on pressure, particularly below 30 MPa. This is due to the presence of thin cracks that close at higher pressures. When relatively incompressible pore fluids, such as water or oil, fill in the pore space, the pores become much less compressible and Vp becomes almost insensitive to pressure. It should also be noted that the Vs increases when the rock is saturated, which is contrary to most other theories.

The Gassmann equation was also used to compute the oil-saturated velocities using the same parameters as in the Toksoz calculations. The dry Vp and Vs for each pressure were also used to provide K_0 . The Gassmann-computed Vp is almost parallel to the dry Vp vs pressure. At low pressure, it drastically underpredicts the saturated Vp (30% lower than the measured Vp at 7 MPa). At higher pressures, the Gassmann predictions agree more favour-

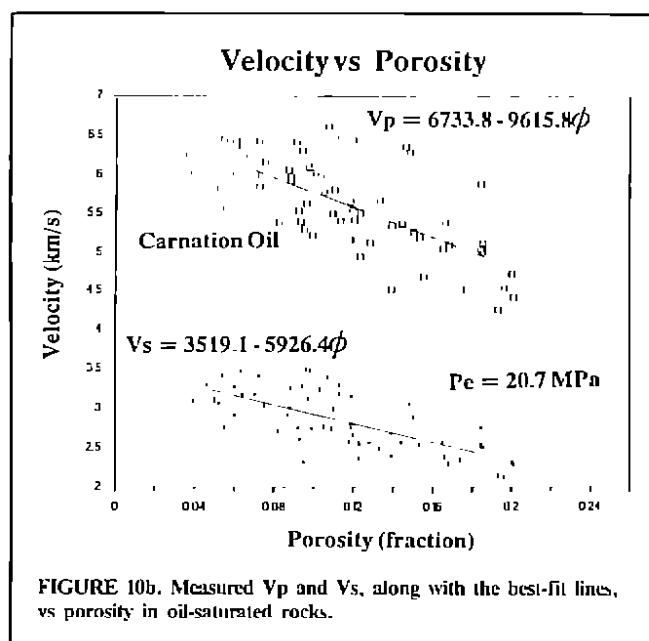
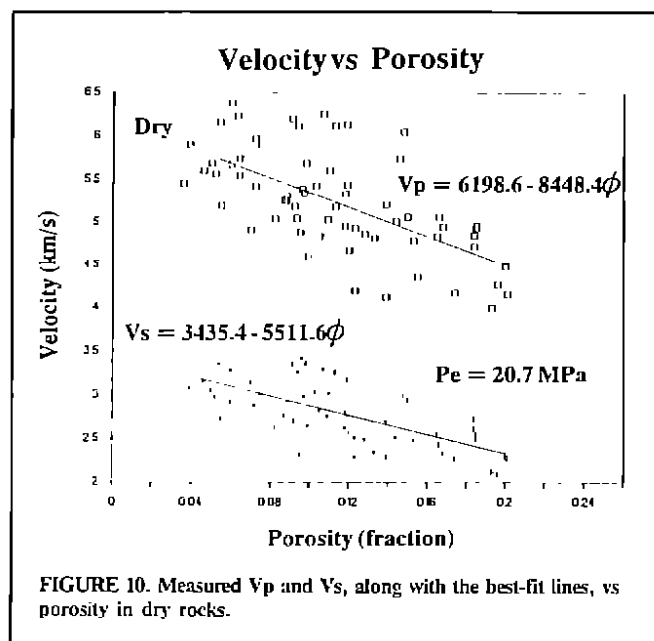
ably with the Toksoz-calculated and measured Vp (-5% deviation at 50 MPa).

Toksoz *et al.* suggested that their model agree with the Gassmann equation when the pores are spherical. In order to test this theory, Toksoz velocities are recomputed using the matrix moduli of the Bedford limestone and an aspect ratio of 1.0. The results showed a decrease of Vp with saturation, which was not consistent with the Gassmann results. The pore geometry was then modified to include 0.1 concentration of spherical pores and 0.03 of aspect ratio 0.1 (for a total porosity of 0.13) and recomputed the velocities. These results are shown and compared with the Gassmann predictions in Figure 8b. In this example, the velocities are only slightly dependent on pressure or saturation. Gassmann prediction of the saturation effect is greater than the Toksoz-calculated values.

These theoretical results are believed to help in interpreting our laboratory data. In general, the results can be broken into three categories regarding the effect of saturation on Vp:

1. Gassmann-predicted Vp change is less than the measured Vp change. This occurs most commonly in samples with dry velocities increasing rapidly with pressure. These rocks show indications of a high concentration of low aspect ratio pores. The majority of these rocks show an increase of Vs when saturated with liquids.
2. Gassmann-predicted Vp change approximately equals the measured Vp change. Samples in this category have moderate increase in dry velocities with increasing pressure. The effect of liquid saturation on Vp is also moderate. Vs usually does not change or decrease slightly when the rocks are saturated with liquids.
3. Gassmann-predicted Vp change exceeds the measured Vp change. These samples often have small and spherical pores. Velocity increase with pressure is often small. The effect of liquid saturation is also small on Vp. Vs decreases as the rocks are saturated with liquids. Pore systems of these rocks tend to be homogeneous without the presence of cracks and low aspect ratio pores.

The Toksoz model provides a reasonable explanation to the disagreement between Gassmann-predicted and measured Vp data. Low aspect ratio pores and cracks are recognized as the most compliant portion of the pore system and have a profound impact on the over-all compressibility and shear strength of the rock, especially at low pressures. As overburden pressure increases, these small cracks are closed and the velocities increase strongly. When these pores are filled with a less compressible liquid, the over-all compressibility decreases greatly so that Vp increases dramatically and becomes less strongly affected by pressure. The use of aspect ratio terms in the Toksoz model allows the calculation of velocities that fit the measured data much better than what is possible with the Gassmann equation.



Initially the authors had hoped to measure the pore aspect ratio spectra for each core sample directly by means of petrographic image analysis (PIA) and use the Toksoz model to calculate the velocities. Unfortunately they were unable to quantitatively match the measured velocities in most cases due to the following causes:

1. **PIA resolution.** The lowest aspect ratio cracks have the greatest impact on the Toksoz-calculated velocities. These cracks are also the hardest to image or resolve in thin section PIA. Even with the scanning electron microscope, it was almost impossible to resolve cracks with aspect ratio lower than 0.02, especially when the image was digitized in the PIA system. In the work published by Toksoz *et al.*, aspect ratio of less than 0.001 (up to 10^{-5}) were used to compute velocities.

2. **Aspect ratio limitations.** The Toksoz model assumes that the pores are non-interactive in the rock. This places a restriction in the model that $c(\alpha_m)/\alpha_m < 1$ [equations (8) to (10)]. It is often observed that $c(\alpha_m)/\alpha_m$ is greater than 1 in thin section analysis. When these pore geometries were input into the Toksoz model, the equations broke down.

In the Toksoz paper, aspect ratios were inverted from velocity data. The difficulty in this approach lies in its non-uniqueness. A set of aspect ratios can satisfy the data but these aspect ratios may not reflect the true pore aspect ratio spectra for the rock.

Discussion

Effect of Pressure

Both V_p and V_s were measured in all the selected core samples at reservoir temperature vs effective pressure ranging from 6.9 MPa to 34.5 MPa which covers the in-situ net overburden pressure range for most Alberta reservoirs. Figures 9a and 9b show the percentage velocity increase in all the dry (air-filled) and oil saturated samples, respectively, as effective pressure increases from 6.9 MPa to 34.5 MPa. This velocity increase with effective pressure is of course nonlinear: the velocities increase faster in the low pressure range, as shown in Figures 4 and 5.

When the core samples are dry or saturated with gas, the compressibility of the pores is relatively high, especially for rocks with low aspect-ratio pores, because the compressibility of the pore fluid is high. As effective pressure increases, some low aspect-ratio pores close to make better contact within the rock's frame and as a result, the compressibility (the inverse of bulk modulus) of the rock decreases and V_p increases. The better contact or the closure of thin pores also increases the rock's ability to resist shear stress so that the shear modulus of, and hence the V_s in, the rock increases.

Figures 9a and 9b also reveal that the percentage velocity increase with increasing effective pressure is essentially independent

of the porosity of the core samples. This may be surprising because, intuitively, pressure increase creates more contacts or pore closures in more porous rocks. However, this velocity increase is not only affected by the porosity, but also by the shape of the pores: when pores in a rock are thin (such as cracks or microfractures) or of low-aspect ratio, the porosity of this rock may be low but the velocities (both V_p and V_s) may increase rapidly with increasing effective pressure because thin pores are easy to close or deform. In this type of rock, V_p increases dramatically when gas in the pores is replaced by a liquid while V_s increases slightly; when the pores in a rock are round-shaped or of high-aspect ratio, the porosity may be high but the velocities may increase only nominally when pressure increases because round pores are hard to close or deform. In this type of rock V_p increases slightly and V_s decreases with liquid saturation⁽¹⁹⁾.

The results also show that the change in velocity with pressure covers a wide range. At a given porosity, the increase in V_p ranges from 2% up to 35%, while the increase in V_s ranges from 1% to 25%. This makes it very difficult in carbonate reservoirs to derive porosity information from velocity-depth relationship.

Effect of Porosity

Figures 10a and 10b show the V_p and V_s in dry and oil-saturated samples, respectively, vs porosity at an effective pressure of 20.7 MPa (3000 psi) and reservoir temperature. The data show that both V_p and V_s decrease as porosity increases. Although there is considerable scatter in the data, the trend is clear.

The relationship between porosity and velocities has been studied by Hamilton⁽²⁰⁾ on unconsolidated marine sediments and by Han *et al.*⁽²¹⁾ on consolidated sandstones, but no systematic studies have been reported for carbonate rocks. In general, both V_p and V_s decrease with increasing porosity in any material. This arises because both the bulk and shear moduli decrease with increasing porosity.

Linear regressions are applied to all the V_p and V_s data. The best-fit lines (solid), along with the best-fit equations are also plotted on the figures. The correlation between porosity and velocity shows a high degree of scatter. This is most evident in dry rocks and at low pressures where pore geometry variations have the greatest impact. At 10 MPa the correlation factor in dry rocks is only 0.57, increasing to 0.76 in oil-saturated rocks. As net pressure is increased to 40 MPa, the correlation factor is 0.70 for dry rocks and 0.81 for oil-saturated rocks. For rocks with mainly round (high-aspect ratio) pores, the velocities are less dependent on porosity than for rocks with cracks (low aspect-ratio pores).

The poor correlation between porosity and velocity or the scatter of the data may also be caused by the composition difference

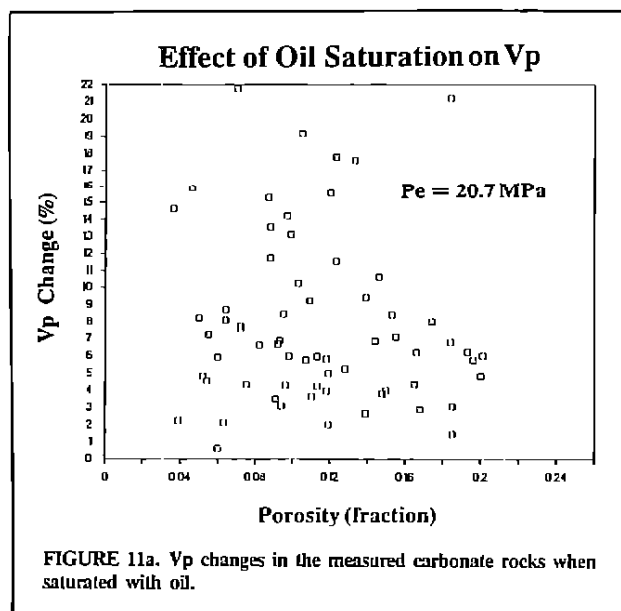


FIGURE 11a. Vp changes in the measured carbonate rocks when saturated with oil.

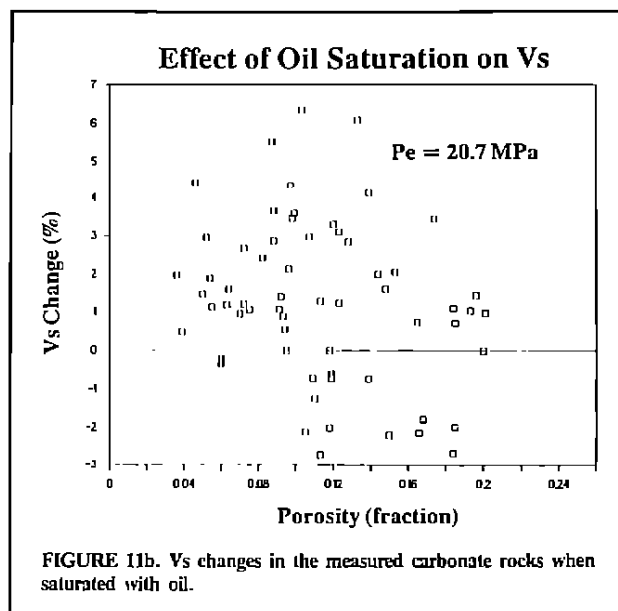


FIGURE 11b. Vs changes in the measured carbonate rocks when saturated with oil.

TABLE 2. Best-fit results for velocity-porosity relations in about 80 carbonate rocks

Saturation	Pe = 6.9 MPa (1000 psi)		Pe = 20.7 MPa (3000 psi)		Pe = 34.5 MPa (5000 psi)	
	Vp (m/s)	Vs (m/s)	Vp (m/s)	Vs (m/s)	Vp (m/s)	Vs (m/s)
Gas-Saturation	5672-8006 ϕ	3260-5533 ϕ	6199-8448 ϕ	3435-5512 ϕ	6446-8440 ϕ	3513-5440 ϕ
Oil-Saturation	6648-10515 ϕ	3392-5959 ϕ	6734-9616 ϕ	3519-5926 ϕ	6806-9332 ϕ	3579-5815 ϕ
Pentane-Flood	6513-13316 ϕ	3363-6819 ϕ	6606-11407 ϕ	3453-6171 ϕ	6683-10669 ϕ	3498-5809 ϕ
Solvent-Flood	6038-11688 ϕ	3257-6103 ϕ	6439-11305 ϕ	3445-6208 ϕ	6512-9825 ϕ	3477-5535 ϕ
Water-Flood	6586-11339 ϕ	3379-6600 ϕ	6690-10342 ϕ	3471-6090 ϕ	6764-10043 ϕ	3529-5890 ϕ

ϕ : Porosity in fraction (from 0.03 to 0.21); Pe: Effective pressure = overburden pressure - pore pressure.

among rocks. The core samples were collected from over 10 carbonate reservoirs and from different wells so that the mineral composition is different. For example, some rocks contain a substantial amount of anhydrite or sand. Dolomites and anhydrite in limestones increase, while sands decrease, the velocities⁽²²⁾.

The velocity data also show that the Vp/Vs ratio increases with increasing porosity in carbonate rocks, in agreement with the results of Castagna *et al.*⁽²³⁾ for clastic rocks and Han⁽²⁴⁾ for sandstones. These Vp/Vs data have become increasingly important in amplitude vs offset (AVO) analysis because the magnitude of the AVO is a measure of Vp/Vs or Poisson's ratio.

Table 2 lists all the best-fit equations for the porosity-velocity relationship for all the core samples when saturated with gas (dry) and oil, and flooded by pentane, hydrocarbon solvent, and water at three effective pressures and reservoir temperature. Note that these best-fit equations apply only in the porosity interval of 0.03 to 0.21.

Effect of Oil Saturation

Figure 11a shows the effect of oil saturation on Vp in the core samples at an effective pressure of 20.7 MPa (3000 psi) and reservoir temperature. Upon oil saturation, Vp in the cores increase by 0.5% to 22%. This Vp increase is caused by the decrease in compressibility: when the air in the pores is replaced by a much less compressible fluid (here oil), the compressibility of the pores decreases dramatically so that the over-all compressibility of the rock decreases. The magnitude of the Vp increase is controlled mainly by the pore geometry. For rocks with mainly round (high aspect ratio) pores, the compressibility of these round pores is low so that the pore compressibility is not very dependent on the type of the pore fluid; for rocks with cracks or microfractures (low aspect-ratio pores), the pores are very compressible when they are empty or filled with gas, but when these low aspect-ratio pores are filled with oil or water, their compressibility decreases dra-

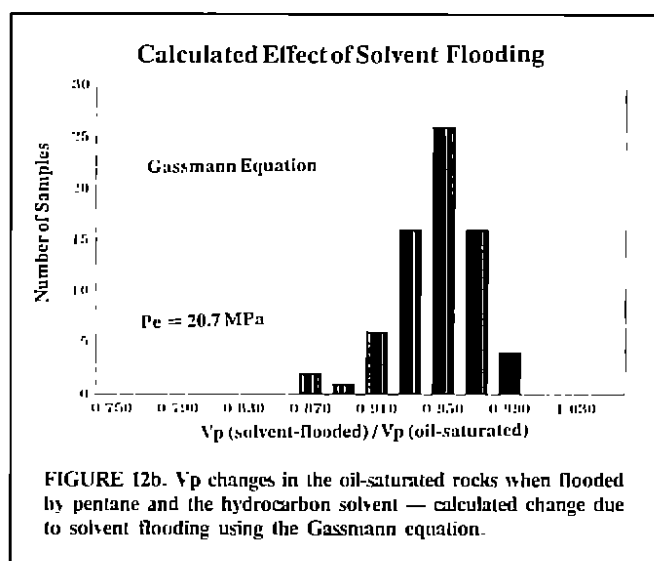
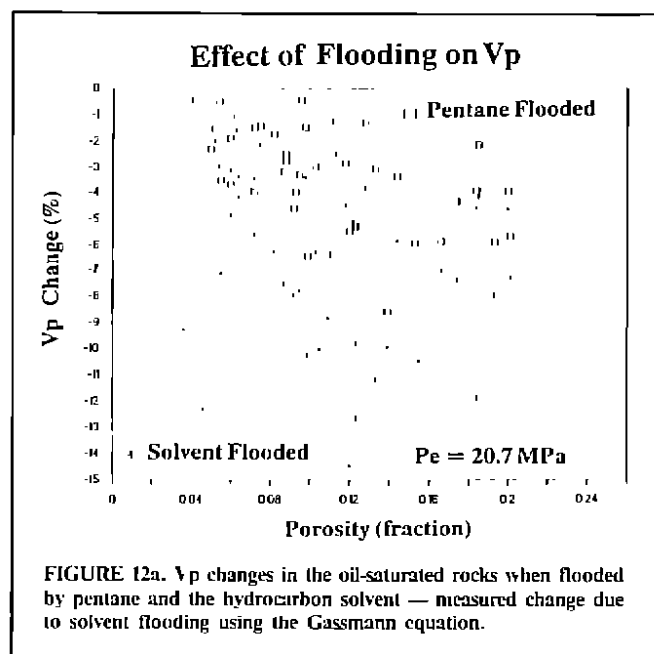
matically, resulting in a lower over-all compressibility and higher Vp for the rock⁽¹⁸⁾.

Theoretically, both the Gassmann equation⁽¹³⁾ and Biot theory⁽¹⁴⁾ show that Vp increases when a porous medium is saturated with a liquid. However, the magnitude of the Vp increase predicted by these theories is usually less than that measured, because these theories do not include the pore geometry variations.

The data in Figure 11a are very scattered. The scatter of the data reflects the complexity of the rock pore geometry. It is very difficult to quantify the relationship of saturation to Vp and pore geometry. The Toksoz *et al.*⁽¹⁸⁾ model takes into account pore geometry but the pore aspect-ratio distribution in this model is usually non-unique as pointed out in the previous section.

Figure 11b shows the effect of oil saturation on Vs. In some cores, Vs increases, by up to 6.5% (with most data below 3%). In some cores, Vs decreases, by up to 3%, with oil saturation.

The increase in Vs as the cores are saturated with oil contradicts the Gassmann equation which predicts that Vs in a liquid-saturated rock is lower than that in the same rock saturated with gases, because neither liquid nor gas supports shear stress (zero shear moduli) and the density of the liquid-saturated rock is higher. However, the measured increase in Vs can be explained by the viscous relaxation theory⁽²⁵⁾ that liquids can support some shear stress because of their viscosity especially when the wave frequency is high. When a rock sample contains pores of low-aspect ratio, the liquid in these pores does not have enough time to relax (or to equilibrate) in the time interval of a half wave period when the viscosity and the wave frequency are high. In this case, these liquid-filled thin pores act like part of the solid matrix of the rock, so that Vs is higher⁽⁴⁾. The magnitude of the Vs change is controlled by the pore aspect ratio, the crack density, and the porosity of the rock, the viscosity and density of the pore fluid, and wave frequency. This could also explain the scatter in the data in Figure 11b. The Toksoz model



also shows that when the rock contains mainly round pores, Vp decreases, but when the rock contains low aspect-ratio pores, Vs increases, as the rock is saturated with a liquid (Figs. 8a and 8b).

The magnitude of the changes in both Vp and Vs upon oil saturation is also controlled by the effective pressure. At low effective pressures, the effect of oil saturation on both Vp and Vs is high (figures not shown) because most low aspect-ratio pores are still open. At high pressures, many thin pores are closed so that the effect of saturation is smaller.

Effect of Pentane and Solvent Floodings on Vp

Once the velocity measurements were complete in the oil-saturated samples, the cores were flooded with pentane, followed by the hydrocarbon solvent. Figure 12a shows the effect of pentane and solvent on Vp at an effective pressure of 20.7 MPa and reservoir temperature. Pentane decreases the Vp by 0.5% to 8.5%, and solvent decreases the Vp by 1.5% to 14.5%. The decreases in Vp are due mainly to the increased compressibility of the pore fluids (and hence of the core samples). Both pentane and the hydrocarbon solvent are much more compressible than the oil. The reservoir temperature for most of the measured cores is higher than 56°C, which means that at the pore fluid pressure of 13.8 MPa (2000 psi), the injected hydrocarbon solvent is in the gaseous phase. The compress-

sibility of gases is usually orders of magnitude higher than that of liquids.

Like all other Vp data, the data in Figure 12a are again very scattered. This scatter is caused by the pore geometry heterogeneity, with different rocks having very different pore geometry and crack content, even though the porosity may be the same.

The magnitude of the Vp decrease caused by pentane and solvent is also dependent on the effective pressure: as effective pressure increases, the effect of flooding decreases. For example, at an effective pressure of 6.9 MPa (1000 psi), pentane flooding decreases the Vp by 0.5% to 11% and solvent decreases the Vp by 2% to 24%. When effective pressure increases, some thin pores or cracks are closed or partially closed, so that the compressibility of the rock becomes less sensitive to the changing pore fluids and pore-fluid compressibility.

Figure 12b shows the effect of solvent flooding calculated by the Gassmann equation. The Gassmann equation predicts that in the majority of the measured carbonate rocks, the solvent flooding should lower the Vp by 5% or more. Therefore, even the Gassmann equation, which usually underestimates the velocities, predicts that it should be possible to use seismic methods to monitor hydrocarbon solvent flooding processes.

Effect of Water Flooding on Vp

The hydrocarbon solvent flooding was followed by water displacements at a constant pore pressure of 13.8 MPa (2000 psi) and reservoir temperature to simulate waterflooding processes. Figure 13a shows the Vp changes caused by the waterflood. The waterflooded Vp was compared to that for the same cores when first saturated with oil and then flooded with pentane. In general, the Vp difference between waterflooded and oil-saturated cores is very small, ranging from -2% to 3%, while that between waterflooded and pentane-flooded cores ranges from 0.5% to 8% (with the exception of one core).

Figure 13a shows that Vp in some oil-saturated cores is decreased when the cores are flooded with water. Theoretically, Vp in water-saturated rocks should be higher than that in the oil-saturated rocks because water is less compressible than the oil. The explanations for the lower Vp in the waterflooded cores are that (1) there may be some trapped hydrocarbon solvent in the cores which is not displaced by the injected water, and (2) even after pentane, the hydrocarbon solvent, and waterfloods, some oil may still be trapped in the thin pores. After waterflooding, the density of the rock increases (water is heavier than the oil) while the compressibility remains essentially the same as that of oil-saturated case, so that the net effect is decrease in Vp. The Vp is higher in the cores when waterflooded than when pentane-flooded, because water is less compressible than pentane.

Figure 13b shows the calculated effect of waterflooding on Vp in the carbonate rocks saturated with a 35° API oil by the Gassmann equation. For almost all the rocks, waterflooding only increases the Vp by 0 to 3%, according to the Gassmann equation. This means, unfortunately, that seismic methods may have very limited application in monitoring of waterfloods in carbonate reservoirs.

Error Analysis

In the velocity measurements, error might arise from uncertainties in picking the first arrival time of the waves, measuring the sample length, and controlling temperature and pressures. The estimated total error in the velocity values is less than 1% for Vp and 2% for Vs. Because most carbonate rocks are of low attenuation, the first arrivals of both compressional and shear waves are very sharp and clear. The end-surfaces of the cores samples were finely ground to parallel during sample preparations so that the uncertainty in measuring sample lengths is less than 0.2%. The uncertainty in sample length measurement does not affect the effects of oil saturation, pressure, and pentane, solvent, and waterfloodings on the velocities because the same sample was used for velocity measurements. Temperature and pressure were controlled within $\pm 0.1^\circ\text{C}$ and $\pm 0.1 \text{ MPa}$, respectively.

Applications

Mechanical Properties of Carbonate Rocks

The bulk, shear, and Young's moduli and the Poisson's ratio can be derived directly from the Vp and Vs. These dynamic mechanical properties of rocks are very important in many engineering applications such as well completion, borehole stability study, and hydraulic fracturing. Furthermore, the compressive strength of rocks can be derived from the correlations with Young's modulus.

Porosity Determination from Velocities and Sonic Log Calibration

In sonic logging, velocities are used to determine porosities of rocks. The time-average equation⁽¹²⁾ used in sonic log interpretation is over-simplified and often gives substantial amount of uncertainty in the derived porosity. Laboratory-measured velocities can, therefore, be used to calibrate sonic logs. The velocity-porosity relationships shown in Figure 10 and Table 2 can be used as a tool in sonic log interpretation and porosity determination.

Delineating Reservoir Fluids and Monitoring Gas Cap using Seismic Methods

Figure 11a shows that oil saturation increases Vp in all the carbonate core samples. This Vp increase is the physical basis for using seismic methods to delineate gas saturation from liquid (oil or water) saturation in reservoir rocks. Furthermore, because of the Vp contrast between gas- and oil-saturated rocks, seismic methods can be used to monitor the formation, growth, movement, and shrinkage of gas caps.

Seismic Monitoring of Hydrocarbon Solvent Floods

Seismic modelling has shown that in order to use seismic methods to successfully monitor hydrocarbon solvent floods, at least a 5% velocity decrease is needed in rocks upon the hydrocarbon solvent flooding⁽⁹⁾. Figure 12a reveals that Vp decreases by more than 5% in 75% of the oil-saturated core samples when flooded with the hydrocarbon solvent at effective pressure of 20.7 MPa and reservoir temperature. At effective pressure of 6.9 MPa, such Vp decrease is more than 5% in almost all the core samples. As a consequence, seismic methods might be used to monitor the hydrocarbon solvent flooding process, to track the movement of the solvent bank, and to map the solvent-flooded zones in reservoirs. Such monitoring, tracking, or mapping is very important because it improves the solvent flooding economics by allowing the engineer to better control the displacement process and to modify the design promptly when early breakthrough is detected. Details of this application can be found in Hirsche *et al.*⁽⁹⁾.

Seismic Monitoring of Waterfloods?

Figures 13a and 13b show that the difference between the Vp in oil-saturated and waterflooded core samples is usually small, 3% or less. This suggests that seismic methods cannot resolve this Vp difference and, therefore, they cannot be used to monitor waterfloods in carbonate oil reservoirs. For pentane-saturated rocks, the Vp increase is less than 5% in more than half of the measured cores after waterflooding. For some cores, the Vp increase is higher than 5%, but pentane represents an extremely light hydrocarbon (with an equivalent API gravity of 95°) which is seldom found in situ.

The experimental results do show, however, that the Vp difference is more than 5% between the dry and waterflooded rocks in most of the cores, which means that seismic methods might succeed in monitoring waterflood or aquifer water-drive in gas reservoirs.

Summary and Conclusion

Seismic velocities (both Vp and Vs) were measured in the laboratory in over 80 carbonate core samples from more than 10 reservoirs in Alberta. These velocities are measured at reservoir

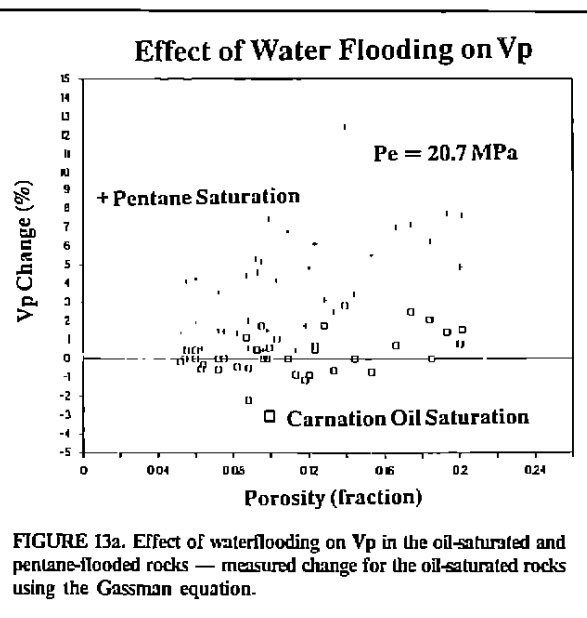


FIGURE 13a. Effect of waterflooding on Vp in the oil-saturated and pentane-flooded rocks — measured change for the oil-saturated rocks using the Gassman equation.

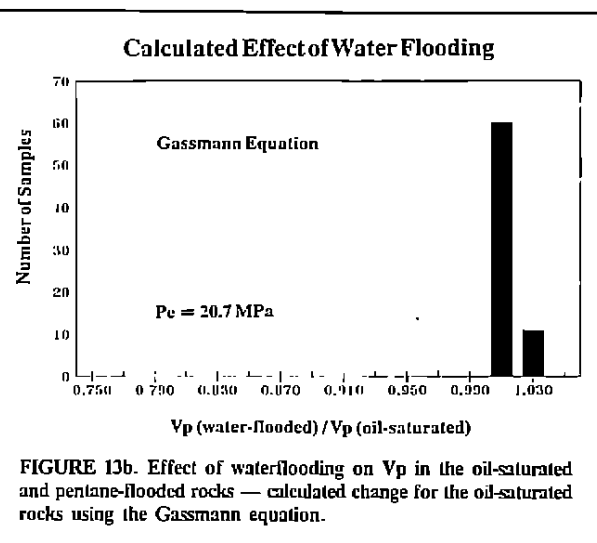


FIGURE 13b. Effect of waterflooding on Vp in the oil-saturated and pentane-flooded rocks — calculated change for the oil-saturated rocks using the Gassman equation.

temperatures (ranging from 23°C to 103°C) vs effective pressure. The effects of porosity, effective pressure, oil saturation, and pentane, hydrocarbon solvent, and waterfloods on the velocities are analyzed, interpreted, and discussed. The complete velocity data, along with other physical properties such as electrical properties (formation factor, cementation exponent, saturation exponent, resistivity index), porosity, air and liquid permeabilities, results of petrographic image analysis (pore structure and geometry, pore size distribution, pore morphology), and capillary pressure data were compiled into a database.

All the velocities increase with increasing effective pressure because higher effective pressure creates better contacts within the rock matrix and closes some low-aspect ratio pores (e.g. cracks and microfractures). Full saturation with an oil increases the Vp but does not affect the Vs much.

As porosity increases, both Vp and Vs decrease. The velocity data are best-fit to some linear relationships between velocity and porosity. This linear correlation is usually poor, with correlation factors ranging from 0.67 for dry rocks to 0.81 for saturated rocks, which means that other intrinsic properties of the rocks also affect the velocities, such as the pore geometry and mineral composition.

The hydrocarbon solvent flooding of the oil-saturated cores decreases the Vp. Seismic modelling shows that a minimum of 5% Vp decrease is probably needed in order to use seismic methods to monitor hydrocarbon solvent floods. Laboratory results show

that at an effective pressure of 20.7 MPa (equivalent to an approximate reservoir depth of 2 km) and reservoir temperature, such Vp decrease is over 5% in about 75% of the measured cores. At an effective pressure of 6.9 MPa (equivalent to an approximate reservoir depth of 700 m), the Vp decrease is over 5% in about 90% of the cores. Therefore, seismic methods may be applicable in many carbonate reservoirs to monitor the hydrocarbon solvent flooding processes, to track the solvent bank, and to map the flooded zones.

The results show that the Vp difference between oil-saturated and waterflooded cores is relatively small, always less than 5%, which means, unfortunately, seismic methods may not be able to monitor waterflood processes in carbonate reservoirs, unless the oil is extremely light (similar to pentane).

Acknowledgment

The authors would like to thank the management of Western Atlas Canada and the Alberta Research Council for the approval to publish this paper, M. McSwiney for carrying out part of the laboratory measurements, and three anonymous reviewers for their helpful and encouraging comments. This paper is part of the results of the project "Seismic monitoring of miscible/immiscible floods" co-funded by Western Geophysical and the Alberta Research Council.

REFERENCES

1. WANG, Z., and NUR, A., Effect of Temperature on the Seismic Wave Velocities in Sandstones and Sands with Heavy Hydrocarbons; 56th Ann. Internl. Mtg., Soc. Explor. Geophys., Expanded abstracts, 3-5, 1986.
2. TOSAYA, C., NUR, A., VO-THANH, D., and DA PRAT, G., Laboratory Seismic Methods for Remote Monitoring of Thermal EOR; *SPE Res. Eng.*, Vol. 2, pp. 235-242, 1987.
3. WANG, Z., and NUR, A., Seismic Velocities in Tar Sands: The Basis for In-Situ Recovery Monitoring; Proc., 4th Internl. Conf. on Heavy Crude and Tar Sands, Vol. 4, pp. 601-611, 1988.
4. WANG, Z., Wave Velocities in Hydrocarbons and Hydrocarbon Saturated Rocks, with Applications to EOR Monitoring; Ph.D. thesis, Stanford University, California, 1988.
5. WANG, Z., and NUR, A., Wave Velocities in Hydrocarbon Saturated Rocks: Experimental Results; *Geophysics*, Vol. 55, pp. 723-733, 1990a.
6. NUR, A., and WANG, Z., In-situ Seismic Monitoring of EOR; The Petrophysical Basis; SPE Paper 16865, 1987.
7. WANG, Z., and NUR, A., Effect of CO₂ Flooding on the Velocities in Rocks with Hydrocarbons; *SPE Res. Eng.*, Vol. 4, pp. 429-436, 1989.
8. HIRSCH, W.K., and SEDGWICK, G., Miscible Flood Monitoring using Seismic Methods; Presented at the 1989 CSEG/CSPG Joint Mtg., Calgary, Alberta, 1989.
9. HIRSCH, W.K., SEDGWICK, G., and WANG, Z., Seismic Monitoring in Enhanced Oil Recovery; CIM/SPE Paper 90-72, 1990.
10. NUR, A., and SIMMONS, G., The Effect of Saturation on Velocity in Low Porosity Rocks; *Earth Plan. Sci. Lett.*, Vol. 7, pp. 183-193, 1969.
11. RAFAVICH, F., KENDALL, C.H. St. C., and TODD, T.P., The Relationships Between Acoustic Properties and the Petrographic Character of Carbonate Rocks; *Geophysics*, Vol. 49, pp. 1622-1636, 1984.
12. WYLLIE, M.R.J., GREGORY, A.R., and GARDNER, G.H.F., An Experimental Investigation of Factors Affecting Elastic Wave Velocities in Porous Media; *Geophysics*, Vol. 23, pp. 459-493, 1958.
13. GASSMANN, F., Elastic Waves Through a Packing of Spheres; *Geophysics*, Vol. 16, pp. 673-685, 1951.
14. BIOT, M.A., Theory of Propagation of Elastic Waves in a Fluid Saturated Porous Solid, I. Low Frequency Range; II. High Frequency Range; *J. Acoust. Soc. Am.*, Vol. 28, pp. 168-191, 1956a,b.
15. WANG, Z., and NUR, A., Dispersion Analysis of Acoustic Velocities in Rocks; *J. Acoust. Soc. Am.*, Vol. 87, pp. 2384-2395, 1990b.
16. O'CONNELL, R.J., and BUDIANSKY, B., Viscoelastic Properties of Fluid-Saturated Cracked Solids; *J. Geophys. Res.*, Vol. 82, pp. 5719-5725, 1977.
17. MAVKO, G.M., and NUR, A., The Effect of Nonelliptical Cracks on the Compressibility of Rocks; *J. Geophys. Res.*, Vol. 83, pp. 4459-4468, 1978.
18. TOKSOZ, M.N., CHENG, C.H., and TIMUR, A., Velocities of Seismic Waves in Porous Rocks; *Geophysics*, Vol. 41, pp. 621-645, 1976.
19. KUSTER, G.T., and TOKSOZ, M.N., Velocity and Attenuation of Seismic Waves in Two-phase Media; Part I — Theoretical Formulations; *Geophysics*, Vol. 39, pp. 587-606, 1974.
20. HAMILTON, E.L., Sound Velocity and Related Properties of Marine Sediments; *J. Geophys. Res.*, Vol. 75, pp. 4423-4446, 1970.
21. HAN, D., Effects of Porosity and Clay Content on Acoustic Properties of Sandstones and Unconsolidated Sediments; Ph.D. thesis, Stanford University, California, 1987.
22. GARDNER, G.H.F., GARDNER, L.W., and GREGORY, A.R., Formation Velocity and Density — the Diagnostic Basics of Stratigraphic Traps; *Geophysics*, Vol. 39, pp. 770-780, 1974.
23. CASTAGNA, J.P., BATZLE, M.L., and EASTWOOD, R.L., Relationship between Compressional-wave and Shear-wave Velocities in Clastic Silicate Rocks; *Geophysics*, Vol. 50, pp. 571-581, 1985.
24. HAN, D., NUR, A., and MORGAN, F.D., Effects of Porosity and Clay Content on Wave Velocities in Sandstones; *Geophysics*, Vol. 51, pp. 2093-2107, 1986.
25. THURSTON, R.N., 1964. Wave Propagation in Liquids; in *Physical Acoustics*, W. Mason, ed., 1A, Academic Press, 1964.